UNIVERSITY OF CALIFORNIA,
IRVINE

Deconstructing Demand: the Anthropogenic and Climatic Drivers of Urban Water Consumption

THESIS

submitted in partial satisfaction of the requirements
for the degree of

MASTER OF SCIENCE

in Civil and Environmental Engineering

by

Azadeh Hemati

Thesis Committee:
Professor Stanley B. Grant, Chair
Professor David L. Feldman
Assistant Professor Amir Aghakouchak

2016

DEDICATION

To

my parents and friends

in recognition of their worth

an apology

A feeling bears on itself the scars of its birth; it recollects as a subjective
emotion its struggle for existence;
it retains the impress of what might have been, but is not.

Alfred North Whitehead
Process and Reality

and hope

If the fool would persist in his folly he would become wise.

William Blake
"Proverbs of Hell"

TABLE OF CONTENTS

LIST OF FIGURES

ACKNOWLEDGMENTS

I would like to express the deepest appreciation to my committee chair, Professor Stanley Grant, who has the attitude and the substance of a genius: he continually and convincingly conveyed a spirit of adventure in regard to research and scholarship, and an excitement in regard to teaching. Without his guidance and persistent help this dissertation would not have been possible.

I would like to thank my committee members, Professor David Feldman and Professor Amir Aghakouchak, whose work demonstrated to me that concern for global affairs supported by an "engagement" in comparative literature and modern technology should always transcend academia and provide a quest for our times.

In addition, a special thank to Dr. Megan Rippy, whose contribution in stimulating suggestions and encouragement, helped me to coordinate my project especially in writing this thesis.

This work was funded by the National Science Foundation's Partnerships In Research and Education (PIRE) program (OISE-1243543).

ABSTRACT OF THE THESIS

Deconstructing Demand: the Anthropogenic and Climatic Drivers of Urban Water Consumption

By

Azadeh Hemati

Master of Science in Civil and Environmental Engineering

University of California, Irvine, 2016

Professor Stanley B. Grant, Chair

As global populations grow and climate becomes more extreme, cities in drought prone regions of the world such as South East Australia are faced with escalating water scarcity and security challenges. Approaches geared towards addressing these challenges are diverse, and detecting "success" against background climate variability is difficult. Here we use 72 years of urban water consumption data from Melbourne, Australia, a city that recently overcame a 12 year "Millennium" drought, to 1) evaluate the utility of wavelet-based approaches for deconstructing climatic and anthropogenic drivers of urban water demand and 2) assess the relative contribution of various water saving strategies to overall demand reduction during the Millennium Drought. Our analysis points to conservation behavior as a dominant driver of municipal water savings (~69%), followed by non-revenue water reduction (~29%), and potable substitution with alternative sources like rain or recycled water (~3%). Demand exhibited both climatic and anthropogenic signatures, with temperature and rainfall impacting consumption significantly at all frequencies except 0.09-0.2 cpy. Residual patterns in demand (after removing climate effects) mapped to anthropogenic controls like outdoor water restrictions, which damped seasonal variability in consumption during the Millennium Drought, and changing

technologies/social norms, which impacted consumption at sub annual frequencies, particularly from 1960-1990.

INTRODUCTION

As of 2012, approximately 93 million people live in areas subject to severe year-round water scarcity, with upwards of 2.4 billion experiencing scarcity at least one month per year [**Oki and Kanae, 2006; Hoekstra *et al*., 2012**]. While all continents are affected, the most severe water shortages are apparent in Australia, Asia (particularly China and India), the western United States, and parts of Mexico [**Hoekstra *et al*., 2012**]. Indeed, despite the promise of a record breaking El Nino in 2015/2016, the state of California (U.S.) is experiencing its worst drought in over a century, with 51 counties presently listed as primary natural disaster areas and another 7 qualifying for natural disaster assistance [**USDA 2016**]. A similar story is playing out in Perth, Western Australia, which remains in a water vulnerable state (running two desalination plants at full capacity to meet public water demand), despite the cessation of drought in 2009, which failed to bring rain to drought-parched western catchments [**Radcliffe, 2015; Legislative Council Secretariat 2015**]. Indeed, where Australia is concerned drought-induced water scarcity is unlikely to abate in the near future. Climate model projections indicate a warmer, drier, future for both Southwest and Eastern Australia [**Sheffield *et al*., 2012; Dai 2012**], which will place cities in these regions under increased water stress, and has the potential to shift water supply systems from generally robust to predominantly insecure [**Turner *et al*., 2014**].

As we prepare to enter an era of increased water scarcity, a premium must be placed on understanding the factors driving water consumption (both climatic and anthropogenic) to promote efficient water use. In this vein, a variety of studies have explored drivers of water demand, including meteorological variables like rainfall, temperature, and evaporation [**Zhou *et***

***al*., 2000; Adamowski *et al*., 2013; Haquea et. al. 2015**], socioeconomic variables, such as population, household income, and water price [**Zhou *et al*., 2000; Haquea et. al. 2015**], and other anthropogenic variables related to water policy, and water use behavior [**Low *et al*., 2015; Haque *et al*., 2014; Haquea et. al. 2015**]. Much of this work has utilized traditional multiple linear regression models, auto-regressive moving average models, trend-extrapolation, Fourier analysis, or artificial neural networks for evaluating relationships between demand and climatic or anthropogenic drivers [**Zhou *et al*., 2000; Adamowski *et al*., 2013; Tiwari and Adamowski, 2015**]. However, more recently, wavelet analysis has been promoted as a means for assessing these relationships (particularly between meteorological variables and water demand). The key advantage of wavelets is that they allow for synchronous identification of transient relationships between variables at multiple frequencies and times, whereas most other methods operate under the assumption of stationarity [**Grinsted *et al.*, 2004; Adamowski *et al*., 2013; Tiwari and Adamowski, 2015**].

At this point only a few studies have used wavelets to identify coherent patterns in water demand, most notably **Adamowski *et al*., 2013**, who revealed high annual coherence between rainfall, temperature, and water consumption in Calgary, Canada (suggestive of strong seasonality in outdoor water use). However, wavelet analysis is more commonly used in the hydrological, geophysical, ecological, and climate sciences, where it is often paired with multiple linear regression (MLR) models to facilitate identification of frequency and time-specific drivers of environmental pattern [**Keitt *et al*., 2005; Westra *et al*., 2006**]. Our study employs this combined approach (MLR plus wavelet analysis) for the first time to deconstruct the climatic and anthropogenic drivers of urban water consumption in a city with a long history of urban water scarcity, Melbourne, South East Australia. The intent of this work is twofold 1) to illustrate the

utility of a transferable method for evaluating demand (broadly applicable across cities) and 2) to explore the relative contribution of specific climatic or anthropogenic factors to total water savings in Melbourne (findings which are likely to be city-specific).

This paper is organized in two parts, the first of which focuses on Melbourne's recent Millennium Drought and identifying urban water practices that contribute most substantively to water savings during the drought. Subsequently, we look broadly over Melbourne's urban water history, which spans multiple droughts between 1940−2012, and use wavelet analysis and MLR to determine the prevailing climactic and anthropogenic drivers of demand at different times and frequencies. Care is taken to 1) characterize coherent patterns between climate variables and consumption, and the evolution of their phasing over time, and 2) map transient events in residual consumption (e.g., following removal of climate-driven patterns) back to likely anthropogenic drivers of consumption with characteristic frequencies and/or temporal signatures.

CHAPTER 1: STUDY AREA: MELBOURNE AUSTRALIA

Urban Water Supply

Melbourne, the capital city of Victoria, Australia has a population of ~ 4.3 million people, and sources its drinking water from a series of protected catchments located to the north and north-east of the city (green symbols in **Fig. 1a**). Melbourne's catchments cover a total area of ~156,700 hectares, including 56,300 hectares of state forest, 90,800 hectares of national park, 7,500 hectares of Melbourne Water land, and 2,100 hectares of private land. Water from these catchments is stored in 10 major reservoirs with a total storage capacity of 1,812 GL [**Viggers *et al.*, 2013**]. The largest of these reservoirs, the Thomson reservoir, was constructed in 1984, and holds ~60% of Melbourne's total water supply [***van Leeuwen, 2015***] (**Fig. 1a**).

Melbourne's stored reservoir volume is managed by a water wholesaler, Melbourne Water, who is responsible for 1) ensuring its quality and 2) partitioning it between environmental flows and water for urban consumption. Water for the latter category is transferred to three water retail authorities (City West Water, Yarra Valley Water, and South East Water), who are responsible for delivering it to consumers (e.g., homes and businesses within the greater Melbourne Metropolitan Area) (**Fig. 1b**). The two largest retailers, Yarra Valley Water and South East Water, have service areas of 4000 and 3640 km^2 respectively, and each service ~1.7 million people [**Pilgram, 2006**]. City West Water is smaller in scale, with a service area of ~ 580 km^2 and a service population of 0.85 million people [**WSAA Water Services**]. As water is transferred from wholesaler to retailer and retailer to consumer, a fraction is lost as non-revenue

water (NRW) due to physical leaks in pipes, theft, or inaccurate water metering. Although NRW and delivered, billable water are tracked separately by each retailer, both are part of the total urban water consumption for Melbourne reported by Melbourne Water (see red star in **Fig. 1b**).

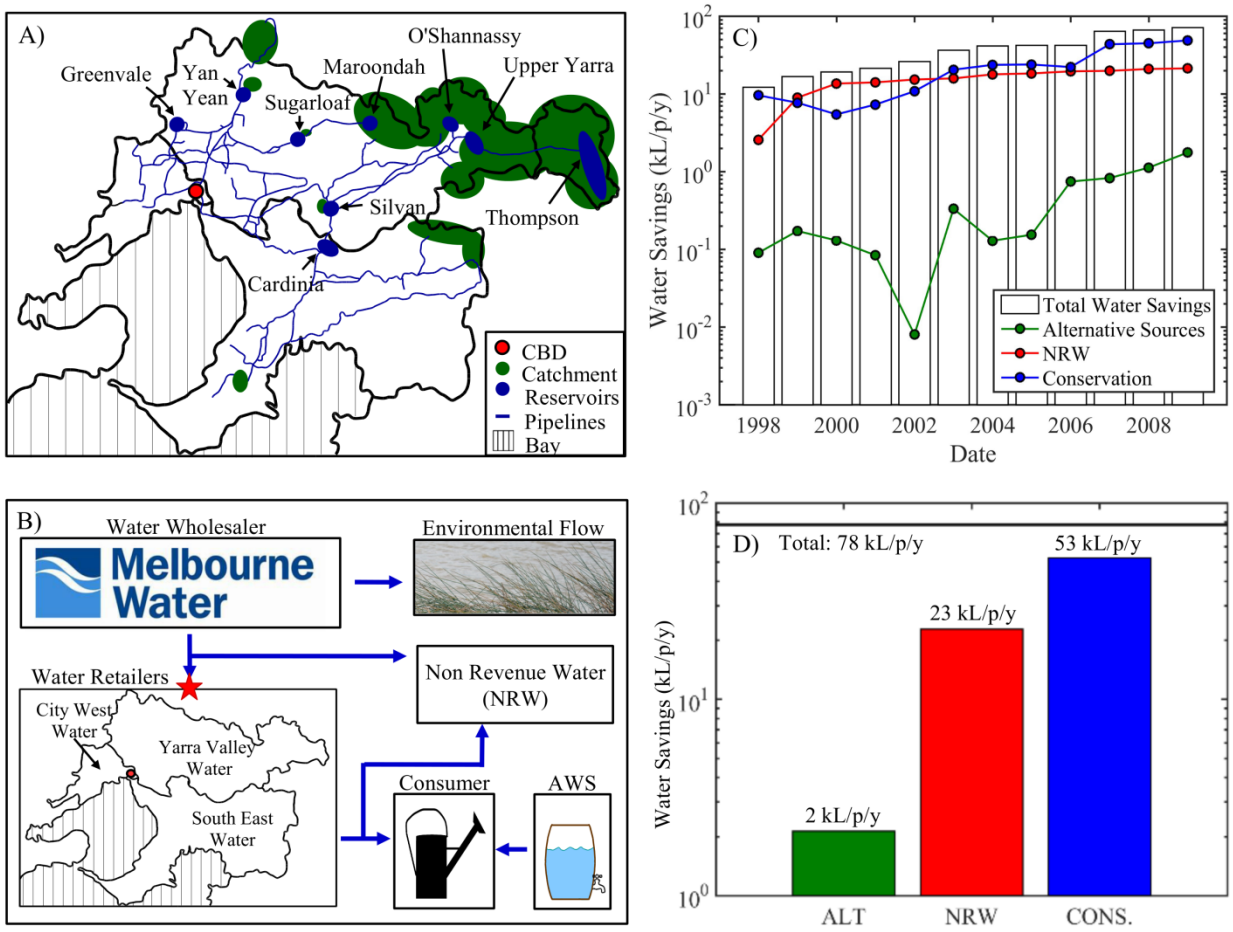

Figure 1: **(A)** Map of Melbourne's water supply catchments detailing catchment bounds (green) reservoirs (blue), and Melbourne's city center, the Central Business District (CBD; red), (**B**) Water management flow diagram (from wholesaler to consumer). The red star denotes the water sold to retailers by Melbourne Water, which includes both non-revenue and billable water. Timeseries of urban water savings during (**C**) and at the end (**D**) of the Millennium Drought (1997-2009), including total savings (black), savings from alternative water sources (green), savings from non-revenue water reduction (red), and savings from conservation behavior (blue).

Drought in SE Australia

Since 1930, Melbourne has experienced 3 long term droughts lasting > five years each (the Second World War Drought: 1937-1945, the 1960's Drought: 1962-1968 (most intense in 1967/1968), and the Millennium Drought: 1997-2009), as well as 2 short term droughts ~ 1 year in duration (the Dust Cloud Drought: 1982-1983, and the 1990's Drought: 1994-1995) [**Helman, 2009**]. Practically speaking, this means that ~50% of the past 82 years in SE Australia have been dry, suggesting that drought, particularly prolonged drought, is a persistent feature of SE Australia's climate. While the Millennium Drought has been called one of the most severe droughts in recent memory [**LeBlanc *et al*., 2009**], it is notable that its spatial extent was smaller and its maximum precipitation deficit lower than both the Federation Drought (early 1900's) and the Second World War Drought, perhaps reflecting different dominant climate drivers [**Verdon-Kidd and Kiem, 2009**]. This said, the Millennium Drought is both the hottest on record, and associated with the lowest inflows in the Murray Darling Basin (the breadbasket of Australia) ever recorded [**Cai *et al*., 2008, Aghakouchak *et al.,* 2014**]. Furthermore, in Melbourne itself, the impact of the Millennium Drought on the annual rainfall deficit was actually larger than other droughts, making its impact on the urban water supply keenly felt [**Verdon-Kidd and Kiem, 2009**].

CHAPTER 2: METHODS

The Millennium Drought: A Water Savings Budget for Melbourne

During the Millennium drought, Melbourne trialed a variety of approaches for reducing pressure on their primary storage reservoirs. These approaches targeted alternative water sources (potable and non-potable), non-revenue water, and conservation behavior. To determine the relative utility of each approach for reducing consumption during the drought, we performed a water savings budget for Melbourne from 1997, when the drought began, to 2009, when the drought officially ended. Total per-capita water savings (S_{TOT}) were calculated as:

$$S_{TOT}(t) = \frac{V_R(1997)}{P(1997)} - \frac{V_R(t)}{P(t)} \quad (1)$$

where V_R (GL/y) is the total volume of reservoir water purchased from Melbourne Water by all three retailers each year (red star in **Fig. 1**), and P is the population of urban consumers the retailers service.

In order to estimate the fraction of S_{TOT} caused by increased use of alternative water sources, information concerning their uptake and storage capacity was compiled from **Low *et al.*, 2015**. Although centralized (and potable) supply alternatives were pursued during the drought (e.g., the Wonthaggi Desalination plant and the Sugarloaf pipeline), both projects were completed after the drought ended, and have since contributed minimally (or not at all) to Melbourne's potable supply [**Barnett and O'Neill, 2010, Grant *et al.*, 2013, Radcliffe, 2015**]. A variety of non-potable projects were also pursued, intended to save potable water for required uses such as drinking. These include recycled water schemes (e.g., dual pipe systems for in-

home uses such as toilet flushing), permanent greywater and stormwater harvesting systems (primarily for outdoor irrigation), and rainwater catchment measures (e.g., rain barrels) [**Low *et al*., 2015**]. Of these different measures, rain barrels and recycled water schemes were the most prevalent (and well documented) during the drought [**Low *et al*., 2015, Bloome *et al*. 2016**]. As such, we define alternative water sources as the sum total of these two technologies for the purposes of this paper. We also assume that potable substitution causes a corresponding decrease in potable water use, a reasonable assumption in light of the strict potable water restrictions during the Millennium Drought. Given these assumptions, the fraction of S_{TOT} attributed to alternative source adoption (S_{ALT}) was calculated as follows:

$$S_{ALT}(t) = \frac{V_{RW}(t) + V_{RB}(t)}{P(t)} - \frac{V_{RW}(1997) + V_{RB}(1997)}{P(1997)} \quad (2)$$

where V_{RB} and V_{RW} (GL/year) are estimates of the stored water volume in rain barrels or recycled water schemes, respectively (see **Low *et al*., 2015** for a detailed description of the procedures used to estimate V_{RB} and V_{RW}).

In addition to the above-noted supply augmentation measures, Melbourne also explored a variety of NRW reduction strategies targeting both real (leaks and bursts) and apparent (theft and meter error) water loss. These strategies were intended to reduce waste through improved distribution efficiency, and included 1) zone metering programs, where flow meters installed across the water supply network were used to quantify zone-specific NRW, and prioritize leak repair, 2) altered burst repair protocols, where saving water during bursts was prioritized over continuity of customer service, and 3) water meter replacement programs targeting aging meters, poor quality meters, and incorrectly sized meters, amongst others [**Gan and Purss, Water outlook for Melbourne, 2014**]. The per-capita water savings due to these NRW reduction

measures (S_{NRW}) was calculated as follows:

$$S_{NRW}(t) = \frac{V_{NRW}(1997)}{P(1997)} - \frac{V_{NRW}(t)}{P(t)} \quad (3)$$

where V_{NRW} (GL/y) is the total reported volume of NRW summed across Melbourne's three water retailers. In instances where NRW data from water retailers was incomplete (e.g, in 2009 for South East Water, and 1997 for Central West and South East Water), V_{NRW} was estimated from Yarra Valley reports using the average ratio (1996-2012) of V_{NRW} : Yarra Valley NRW, which was relatively stable at 2.4 GL/year (see **Fig. S1c**).

The third major approach for saving water during the Millennium Drought, conservation, is somewhat more difficult to quantify directly given 1) the myriad of individual programs involved (e.g., mandatory and voluntary water use restrictions, rebate programs for water efficient appliances, school and homeowner water education programs, and a variety of water-wise advertisements featured on television, billboards, radio, and in newspapers [**Low *et al.*, 2015**]), as well as 2) the challenges associated with linking programs to behavioral change and volumetric estimates of potable water saved. For instance, while the water savings associated with certain appliance exchange programs have been tabulated directly (e.g., ~8.67 GL/y from washing machine replacement alone [**Joint Water Efficiency Plan, 2010/2011, Low *et al.*, 2015**]), the effects of other programs, particularly educational ones like "Learn it! Live it!" and "Water Smart Behavior Change" instituted by Yarra Valley Water and Melbourne Water, respectively, remain unknown [**Low *et al.*, 2015**]. Given these challenges we have chosen to define the fraction of total water savings due to conservation (S_C) by difference (e.g., $S_C = S_{TOT} - (S_{ALT} + S_{NRW})$), and have not attempted to compare the relative merits of specific conservation programs.

The Historical Water Record: anthropogenic vs climatic drivers of consumption

In order to evaluate the combined influence of climatic and anthropogenic factors on Melbourne's urban water consumption in the long-term, we utilize an innovative combination of wavelet analysis and MLR. This analysis considers 72 years of Melbourne's recorded water history (monthly averages from 1940-2012), and involves two meteorological datasets (temperature; T and rainfall; R), one hydrological dataset (reservoir inflow; I), and one urban water consumption dataset (C). Consumption data were provided by Melbourne Water (same as above), whereas temperature and rainfall timeseries are from the Australian Water Availability Project. These timseries were generated via a gridded, anomaly-based analysis of data from meteorological stations located in and around Melbourne's major water supply catchments (e.g., the Thomson, Upper Yarra, O'Shannaasy, and Maroondah reservoirs, **Fig. 1a**; details in **Jones *et al.*, 2009**). Reservoir inflows (in contrast) were calculated by difference across all reservoirs (e.g., $I = dS/dt + C$, where t is time, S is reservoir storage (measured by Melbourne Water), C is urban water consumption, and I is reservoir inflow). Because our calculations do not account for additional water sinks such as evaporation, environmental flows and/or spills, actual inflows will exceed our estimates.

Analysis was performed in three parts (detailed separately below) using the wavelet coherence toolbox [**Grinsted *et al.*, 2004**], the wavelet toolbox, and the statistics and machine learning toolbox from Matlab, Matworks, 2015b. All timeseries had a monthly timestep and were de-meaned and de-trended prior to analysis.

Continuous Wavelet Transformation

Continuous wavelet transformation (CWT) was used to characterize frequency and time specific patterns in *R*, *T*, *I* and *C*. CWT, unlike traditional spectral techniques, does not assume that signal periodicities are stationary in time, allowing it to be used to resolve events that are localized or intermittent such as droughts, floods, and disease epidemics [**Johnes *et al.*, 2009, Chopra *et al.*, 2015**]. CWT uses wavelets (in this case the Morlet wavelet) as bandpass filters for a timeseries, where the wavelet is dilated or compressed to resolve the contribution of different frequencies to overall variance [**Torrence and Compo, 1998, Grinsted *et al.*, 2004, Guan *et al.*, 2011**]. By definition, wavelet power is the modulus of the wavelet coefficients that result when a timeseries is convolved with a wavelet function [**Grinsted *et al.*, 2004, Guan *et al.*, 2011**]. Importantly, because all wavelet-based analyses have edge effects associated with the convolution of a continuous wavelet with a finite timeseries [**Guan *et al.*, 2011**], care must be taken to evaluate only the time-frequency region that is "free" of edge effects (i.e., beyond the so-called cone-of-influence (COI), see **Grinsted *et al.*, 2004**).

Regions of significant wavelet power outside the COI were identified as those where power was consistently in excess (e.g., 95% of the time) of the expected power if the signal were red noise (i.e., generated by a first order autoregressive process with lag-1 autocorrelation characteristic of our respective *R*, *T*, *I*, or *C* timeseries, details in SI). All patterns in wavelet power were assessed relative to known climatological or anthropogenic events in Melbourne's water history such as major droughts or reservoir additions, to identify patterns that were consistently associated with specific events.

Wavelet Coherence Analysis

Wavelet coherence was used to identify shared patterns (i.e., correlated regions) between *R*, *T*, *I*, and *C* timeseries, and to explore their phase relationships. By definition, coherence is the ratio of the shared power between two signals (*X* and *Y*) and the product of the power in each individual signal at various frequencies and times [**Torrence and Webster, 1998; Grinsted *et al*., 2004; Guan *et al*., 2011**]. This makes it analogous to a localized correlation coefficient in time-frequency space (0: no coherence, and 1: perfect coherence between signals [**Grinsted *et al.*, 2004**]). Wavelet coherence, like CWT, has associated edge effects and can only be interpreted outside the COI (defined as above).

Phase relationships between *R*, *T*, *I*, and *C* were estimated for regions of significant coherence (defined relative to an AR1 red noise process, see SI) using the complex argument of the cross wavelet transform, where phase angle is defined as the arc tangent of the imaginary component of the transform divided by the real component [**Rosenblatt, 1965.; Grinsted *et al*., 2004**]. Phase angles were translated into monthly time lags between *R*, *T*, *I*, and *C* using the following relationship: Time lag = phase angle/$2\pi f$, where f is frequency in cycles per month and the phase angle is a function of frequency and time. The temporal evolution of phase lags was evaluated to determine if relationships between consumption and climate variables changed over time. Phase relationships were also compared across major drought events (e.g., the Millennium Drought, the 1960's drought, and the Second World War Drought).

Discrete Wavelet Transformation and Multiple Linear Regression

Discrete wavelet transformation (DWT) was used in combination with MLR to construct a best-fit "climate only" model for urban water consumption, allowing information regarding

anthropogenic controls to be assessed through evaluation of the residuals (e.g., modeled – observed consumption). DWT was used in lieu of CWT because it uses non-overlapping wavelet packets to generate unique (non-redundant) wavelet coefficients that are well suited for regression analysis [**Westra et al., 2006**]. Following a six-level (e.g., seven frequency) DWT, MLR was performed at each frequency band (dependent variable: *C*; independent variables: *R*, *T*, *I,* and all pairwise interaction terms). Best-fit frequency-specific models were selected using Akaike's Information Criterion (corrected for small sample sizes), and then compiled into an overall best-fit model for *C*. Subsequently, inverse DWT was used to recover our modeled *C* timeseries. Because CWT provides higher fidelity timeseries decomposition than DWT (facilitating pattern analysis), CWT was performed on both observed and modeled *C* prior to taking their difference and assessing the residual for time-frequency signatures indicative of anthropogenic controls on urban water consumption. A detailed description and flow diagram of our complete DWT and regression procedure (inspired by **Westra *et al*., 2006**) can be found in SI (**Fig. S2a**).

CHAPTER 3: RESULTS

The Millennium Drought

Annual urban water consumption peaked in 1997 at the start of the Millennium Drought (167 kL/p/y) and reached its lowest value in 2011, two years after the drought concluded (86 kL/p/y; **Fig. S1a**). This means that by 2009, when the drought officially ended, total potable water savings exceeded 70 kL/p/y (**Fig. 1c,d**). A small fraction of these overall savings were due to alternative water sources (~ 2 kL/p/y), reflecting increased adoption of rain water barrels (post 2007) and recycled water systems (post 2005) in almost equal measure (**Fig. 1d, S1b**) [**Low *et al.*, 2015**]. NRW savings (all water retailers) totaled ~ 23 kL/p/y by the end of the drought (see **Fig. S1c**), and were initially higher than those from conservation behavior (e.g., between 1999 and 2002 **Fig., 1c**). Post 2002, however, savings from conservation behavior exceeded both NRW and alternative water sources combined, totaling ~53 kL/p/y by the end of the drought.

The Historical Water Record

Frequency and Time-Specific Variability in Climate and Consumption

Although Melbourne's urban water consumption was elevated in 1997 at the start of the Millennium drought, the all-time summer high (1940-2012) occurred earlier (e.g., 1982), and the all-time summer low, later (e.g., 2011) (**Fig. S2b**). Consumption exhibited the most power at annual frequencies (significant at the $p < 0.05$ level), diminishing in strength post 2002 (**Fig. 2a**). Power was also elevated between 1960 and 1990, at frequencies below 0.5 cpy.

Climate variables, like consumption, varied widely between 1940 and 2012, with *R*

ranging from 5.7-399 mm/month (taking on lower values in 1991 than during the Millennium Drought), mean monthly *T* ranging from 3.8-20 ˚C (hottest at the start of the drought in 1997), and *I* ranging from < 0-1700 GL/y (highest after the construction of the Thomson reservoir in 1984) (**Fig. S2c-e**). All three variables exhibit high power at annual frequencies, particularly *T* (**Fig. 2e**). Interestingly, *R* exhibits discontinuities in annual power during the Second World War and Millennium Droughts (**Fig. 2d**), whereas *I* exhibits increases in power at all frequencies, coincident with reservoir additions (see vertical black lines**, Fig. 2f**).

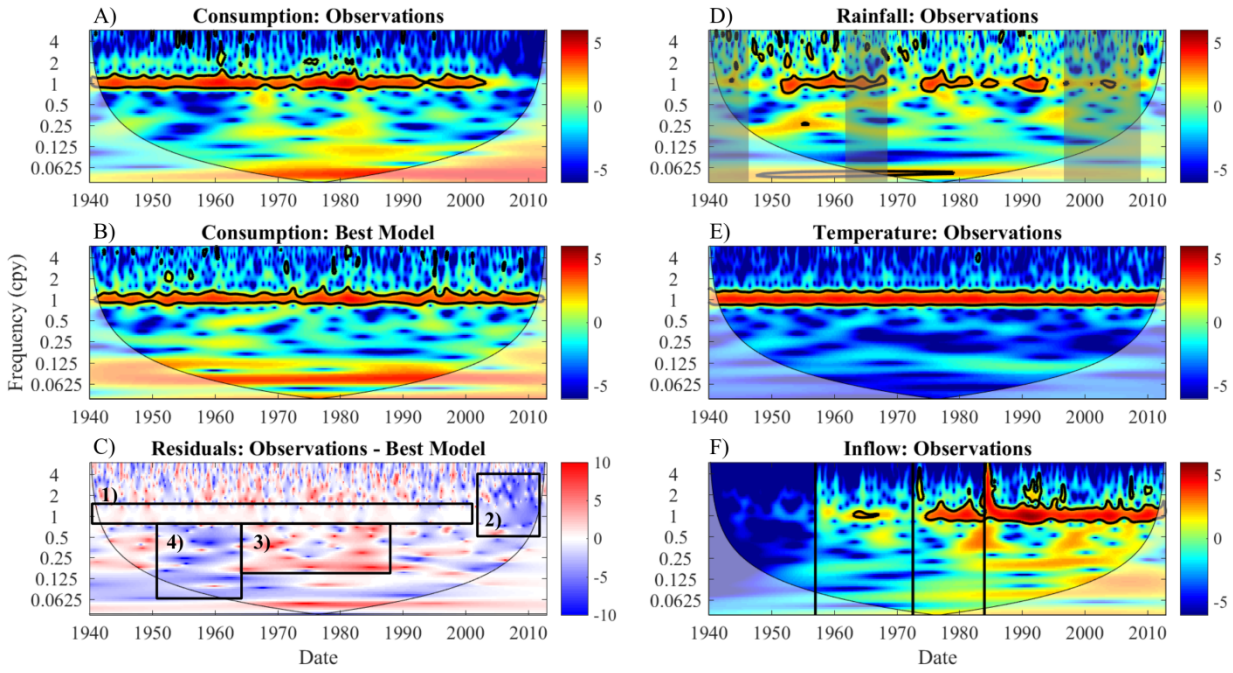

Figure 2: Heat maps of wavelet power for the continuous wavelet transform (CWT) of consumption (**A**), modeled consumption (using a best-fit climate model; **B**), residual consumption (observed – modeled; **C**), rainfall (**D**), temperature (**E**), and inflow (**F**). Black boxes in (**C**) indicate regions of good (box 1) and poor (box, 2-4) fits between observed and modeled consumption. Shaded gray bars in (**D**) indicate long-term droughts, including (from left to right) the Second World War Drought, the 1960s Drought, and the Millennium Drought. Black vertical lines in (**F**) mark large reservoir additions (e.g., capacity exceeding 200 GL), including (from left to right) the Upper Yarra, Cardinia, and Thomson reservoirs. Time (years) is on the *x*-axis, and frequency (cpy) is on the *y*-axis for all panels. Thick black contours denote regions of significant power ($p < 0.05$ level), and white shading (e.g., the cone of influence) indicates regions where estimates of wavelet power are unreliable.

Patterns in Wavelet Coherence and Phase Relationships

Significant coherence was observed at annual frequencies for all possible pairings of *R*, *T*, *I*, and *C*, consistent with the high power annual band observed for each timeseries (**Fig. S3**). Annual coherence was persistent (detected > 70% of the time across all timeseries pairs), and was highest between *T* and *C* (coherent 99% of the time) and lowest in pairings with *I* (coherent 74-79% of the time). Significant coherence was also detected at sub-annual frequencies (e.g., 0.25 and 0.125 cpy), but only transiently. Sub-annual coherence was largest between *I* and *R*, and increased over time (from ~1 cpy pre 1957 to 0.125 cpy by 1995; **Fig. S3d**). Sub-annual coherence between *R* and *T* also changed over time (from ~ 0.25 cpy before 1970 to 0.125 cpy post 1970; **Fig. S3a**).

Given that significant coherence was most consistently detected at annual frequencies, our exploration of phase relationships between *R*, *T*, *I*, and *C* was limited to the annual band. On average, *T* and *C,* and *R* and *I* were in phase (0.1 +/- 0.2 and 0.4 +/- 0.5 month lag, respectively; the pair *R* and *I* lead the pair *T* and *C* by ~ 5 months (**Fig 3b, Table S1**). However, phase relationships between variables were not constant, and exhibited small, but significant ($p < 0.01$), trends (statistical details in SI). For instance, the lag between *R* and *I* increased over time (total change of ~½ months between 1940 and 2012), whereas decreasing lags of similar magnitude were observed between *R* and *T*, *R* and *C*, *I* and *T*, and *I* and *C* (~½-1 months) (see trend lines**,** **Fig. 3a, Table S1**). Phase relationships for individual droughts generally reflect these trends, with *R* and *I* leading *T* and *C* by the greatest margin during the Second World War Drought, followed by the1960's Drought and the Millennium Drought (**Fig. 3c-e**).

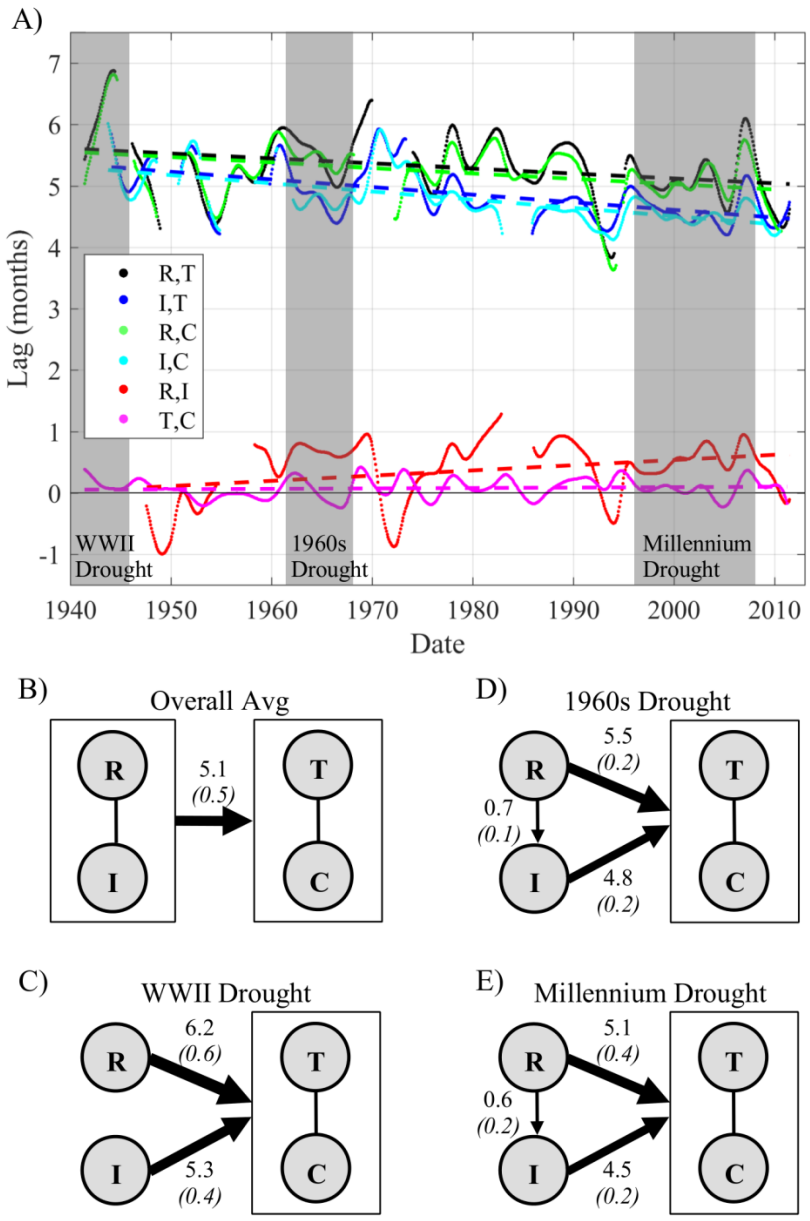

Figure 3: (**A**) Timeseries of significant phase lag (estimated at an annual frequency) between rainfall (*R*), inflow (*I*), temperature (*T*), and consumption (*C*) from 1940-2012. Time (years) is on the *x*-axis, and phase lag (months) is on the *y*-axis. Observed phase relationships (circles; gaps indicate regions where no significant relationship occurred) and long-term trends (dashed lines) are shown in color: *R* leads *T* (black), *I* leads *T* (blue), *R* leads *C* (green), *I* leads *C* (cyan), *R* leads *I* (red), and *T* leads *C* (pink). Grey bars mark individual drought events as in **Fig. 2d**. (**B-E**) Maps illustrating average phase relationships between 1940 and 2012 (**B**), and for individual drought events, including the Second World War Drought (**C**), the 1960s Drought (**D**), and the Millennium Drought (**E**). Arrow widths and associated coefficients indicate the magnitude (+/- *standard deviation*) of the lag. Boxes are used to group model components that are in-phase (e.g., exhibit no significant monthly lag).

Climatic and Anthropogenic Patterns in Urban Water Consumption

Climate variables alone (e.g., *R*, *T*, *I*, and all pairwise interaction terms) explained ~55% of the observed variance in Melbourne's urban water consumption (**Fig. S4**, **Table S2**). Different variables were significant at different frequencies ($p < 0.05$ level). For instance, *R* and *T* were significant predictors of consumption at all frequencies except 0.09 – 0.2 cpy. In the latter frequency band no variable explained more variance in consumption than expected by chance (i.e., the best model was the null model; **see Fig. S4f**). *I* only improved model fits at greater than or equal to annual frequencies, and was never itself a significant predictor of consumption; its inclusion was contingent upon the significance of pairwise interactions with *R* and/or *T*. Importantly, the best-fit frequency-specific models presented here should be interpreted as one possible realization of a family of best-fit models, as their corrected Akaike weights fall between 0.17 and 0.52 (i.e., there is only a 17-52% chance that the models we selected are truly "best"; **Table S2**).

Our final "climate-only" model reproduced patterns in consumption most reliably at annual frequencies (> 80% variance explained), particularly between 1990 and 2002 (see box 1 in **Fig. 2c**). This said, it clearly fails to capture the decrease in annual power observed post-2002 during the Millennium Drought (see box 2 in **Fig. 2c**). The model also over-predicts power in greater than annual frequencies (during the Millennium Drought) as well as in sub-annual frequencies between 1950 and 1965 (see box 4 in **Fig. 2c**). Finally, the model under-predicts power from 1965-1990 at sub-annual frequencies (see box 3 in **Fig. 2c**). Importantly, there are no consistent biases between modeled and observed consumption, but rather a series of transient biases that reflect distinct historical or climatological events unresolved by our climate-only model.

DISCUSSION

During the Millennium Drought demand-side approaches for reducing urban consumption (e.g., conservation: 69%, and NRW reduction: 29%) conferred more benefit than supply-side approaches (e.g., alternative water sources: 3%; desalination plant and Sugarloaf pipeline: 0%) (**Fig. 1d**). Similar success with demand-side techniques has been reported by the city of Cheyenne, Wyoming in 2002, where urban consumption was reduced ~50% in summer months, primarily through outdoor watering restrictions (total savings of 60.2 ML/d), as well as Boston, Massachusetts, where consumption declined ~25% in the early 1990's (and has remained low) primarily due to aggressive leak repair, rebate programs for water saving technologies in the home, and increased efficiency of industrial water use [**Wilhite, 2005 ch7**].

Although conservation saved more water at the end of the Millennium Drought than NRW reduction, the inverse was true between 1999 and 2002 (**Fig. 1c**), suggesting that early investment in NRW programs can have rapid (if diminishing) returns. Furthermore, because pressure/leak management initiatives can reduce utility maintenance costs through extending the lifetime of infrastructure, NRW programs may prove an attractive (even profitable) means of reducing water consumption in the long term [**Girard and Stewart, 2007; van den Berg, 2015**]. Indeed, a pilot study by Gold Coast Water in Queensland, Australia revealed that pressure and leak management initiatives can save upwards of 3.4 million AU dollars per year in maintenance costs, and provide more water savings benefit per dollar than either supply-augmentation (e.g., desalination, dam retrofits, and water supply pipelines) or the sum total of existing water rebate programs [**Girard and Stewart, 2007**].

Although savings from alternative water sources during the Millennium Drought were consistently low, this may (in part) reflect the longer spin-up time required for such projects. Indeed, by 2013/2014 (five years after the drought concluded), $50 million AU dollars had been allocated to building stormwater systems for the purposes of potable substitution, implying that the full effect of these measures is yet to be realized [**Low *et al*., 2015**]. Furthermore, given that many alternative water systems provide benefits beyond supply (e.g., related to water quality, energy savings, and ecosystem/public health), their utility in urban environments is likely to exceed their importance for drought mitigation alone [**Walsh, 2005; Walsh *et al*., 2016; Askarizadeh *et al*., 2015**].

While some of the supply-side solutions implemented during the Millennium Drought were not utilized (e.g., the desalination plant and the Sugarloaf pipeline), they may have afforded the security necessary to innovate, enabling pursuit of less traditional (riskier) demand-side solutions to urban water problems [**Coppock and Brown, 2007**, **Low *et al*., 2015**]). This kind of innovation comes at a cost, however, including 1) the fixed price of infrastructure (AU$ 6 billion for the desalination plant alone [**Grant *et al.*, 2013**]), and 2) any future costs that accrue if infrastructure is maladaptive (e.g., increases emissions of greenhouse gasses, reduces incentives for adaptation, and/or the paths available to future generations [**Barnett and O'Neill, 2010**]). These considerations complicate efforts to quantify the net costs and/or benefits of centralized infrastructure to urban water security in the long term.

Looking beyond the Millennium Drought, there are clear patterns in urban water consumption throughout Melbourne's history (1940-2012), some of which appear driven by meteorological and/or hydrological variables. This is clearly evidenced by the high annual coherence between consumption and climate variables (**Fig. S3**), previously noted by **Zhou *et***

***al*., 2000** (for Melbourne) and **Adamowski *et al*., 2013** (for 3 cities across Canada). High annual coherence points to significant seasonality, with *T* and *C* oscillating in phase (more consumption in warmer summer months), and *R*:*I* being nearly out of phase with *T*:*C* (consistent with the idea that consumption and temperature are highest when rainfall and inflow are lowest) (**Fig. 3**). Interestingly, the phase lag between *R* and *I* in Melbourne appears to have increased slowly but significantly over time, from in-phase around 1950 (peaking in winter/spring) to *R* leading *I* by ~ ½ month in 2012 (**Fig. 3, Table S2**). That is consistent with the findings of **Cai *et al*., 2008** and others, who identified altered *R*-*I* relationships as a key difference between the Millennium Drought and prior mega-droughts like the Second World War and Federation Droughts: essentially, reduced autumn rainfall fails to prime upper soil layers with moisture, resulting in delayed (and reduced) inflow in response to major rain events in winter/spring [see also **Verdon-Kidd and Keim 2009; Ummenhofer *et al*., 2011; van Dijk *et al*., 2013**].

Given the high shared power between climate and consumption at annual frequencies, it is unsurprising that our optimal climate-based consumption model performed best at those frequencies (**Fig. 2c, box 1**). That said, post 2002 the model clearly overestimates the contribution of high frequency variability to urban water consumption (**Fig. 2c, box 2**). This mismatch likely reflects the influence of water conservation programs during the Millennium Drought, as these programs: 1) saved more water post 2002 than other approaches (e.g., NRW reduction and alternative water sources; **Fig. 1c**) and 2) targeted outdoor (as well as indoor) water use, which varies seasonally. Indeed, the first wave of mandatory water restrictions targeting outdoor water use (Stage 1 restrictions) were implemented in November 2002, coincident with the onset of our poor model-data fits. Subsequent stages (implemented in 2003, 2006, 2007, and 2008) only strengthened outdoor watering restrictions, culminating in Stage 3a,

which was one step below a total outdoor watering ban [**Low *et al*., 2015**].

Another notable failure of our climate-only model is evident between 1960 and 1990, where power is underestimated at sub-annual frequencies (**Fig. 2c, box 3**). This timeframe maps to a period of technological innovation and changing social norms regarding water use in Melbourne. For instance, piped hot water became freely available in the home by the mid-1960s paving the way for hot water appliances such as the dishwasher and washing machine, as well as new accepted hygiene practices (most particularly the daily shower) [**Davison, 2008 ch 3**]. These changes, alongside shifts in outdoor watering habits (spurred by suburban sprawl and a preference for backyard lawns) ushered in a new era of high urban water use (see consumption peak in **Fig. S2b**) [**Davison, 2008 ch 3**]. The mid 80's to early 90's, in contrast, mark the start of a more water conservative mindset for Melbourne, including mandatory use of dual flush toilets in new toilet installations (1984), public awareness campaigns like "Don't Be a Water Wally" (1984), and user-pays water pricing regulations (1986) [**Davison, 2008 ch 3; National Water Commission, 2011; Low *et al*., 2015**]. Superimposed on this long term (lower frequency) pattern are two droughts, first in 1968, the worst year of the 1960's drought, and then in 1983, the dust cloud drought (see hotspots at 0.5 cpy in box 3, **Fig 2a,c**). The intense model-data mismatch during these periods likely reflects 1) the short, sharp nature of the droughts themselves, and 2) their occurrence in a era when Melbourne's average water consumption was at an all-time high.

Although our analysis of residual consumption (discussed above) is intended to isolate patterns driven by anthropogenic factors from those driven by climate, it is important to recognize that this separation may be incomplete, as our best-fit "climate" model is unlikely to represent only climate. For instance, our inflow variable *I* (included in best-fit models at greater

than or equal to annual frequencies) is clearly influenced by human modification of the water supply catchment (e.g., reservoir additions), as well as rainfall, making it a hybrid variable (i.e., it reflects both human and climate drivers, **Fig. 2c and S3d**). Similarly, anthropogenic effects on temperature such as global warming could make temperature a hybrid variable, complicating model interpretation. Nevertheless, our combined wavelet and MLR analysis clearly identifies both climatic and anthropogenic factors as important drivers of Melbourne's urban water consumption. The effects of climate were present at nearly all frequencies (not just seasonal, as has been assumed in other studies [**Zhou *et al*., 2000**], see **Fig. S4**), whereas the effects of anthropogenic factors varied: sometimes evident at low frequencies (e.g., between 1960 and 1990), and other times at high frequencies (e.g., during the Millennium Drought).

REFERENCES

1. Adamowski, J.; Adamowski, K.; Prokoph, A. A spectral analysis based methodology to detect climatological influences on daily urban water demand. Math Gosci. 2013, 45, 49-68.

2. Aghakouchak, A.; Feldman, D.; Stewardson, M. J.; Saphores J.; Grant, S. B., and Sanders, B.; Australia's Drought: Lessons for California. *Science.,* 2014, 343(6178), 1430-1431. DOI: 10.1126/science.343.6178.1430.

3. Askarizadeh, A.; Rippy, M. A.; Fletcher, T. D.; Feldman, D. L.; Peng, J.; Bowler, P., Mehring, A. S.; Winfrey B. K.; Vrugt, J. A.; AghaKouchak, A.; Jiang, S. C.; , Sanders, B. F.; Levin, L. A.; Taylor, S., and Grant, S. B.; From Rain Tanks to Catchments: Use of Low-Impact Development To Address Hydrologic Symptoms of the Urban Stream Syndrome. *Environ. Sci. Technol.*, 2015, 49 (19), 11264–11280; DOI: 10.1021/acs.est.5b01635.

4. Bloome, D. W.; Guzman, E., and Jaeckel, D., Transferring lessons from Australia's Millennium drought to California: Accelerating adaptation to drought, flood and heat. *Tree People,* 2016 https://www.treepeople.org/sites/default/files/pdf/publications/TreePeople%20-%20Transferring%20Lessons.pdf.

5. Cai, W., and T. Cowan, Evidence of impacts from rising temperature on inflows to the Murray-Darling Basin. *Geophys. Res. Lett.*, 2008, 35, 1−5.

6. Chopra, S., and Marfurt, K. J.; Choice of mother wavelets in CWT spectral decomposition, SEG Technical Program Expanded Abstracts, 2015, 2957−2961; DOI: 10.1190/segam2015-5852193.1.

7. City West Water, South East Water, Yarra Valley Water, Melbourne Water. Melbourne joint water efficiency plan. Annual Report 2010/2011.

8. Coppock, M. h., and Brown, R. R.; Advancing sustainable water futures for Melbourne: analysis of expert opinion on structural and non-structural approaches. *Water Pract. Tech.* 2007, 2 (2); DOI: 10.2166/wpt.2007.054.

9. Crowley, P. M.; Long cycles in growth: explorations using new frequency domain techniques with US data Bank of Finland Research Discussion Papers, 2010, 6.

10. Dai, A.; Increasing drought under global warming in observations and models. *Nat. Clim. Chang.,* 2013, 3, 52–58; doi:10.1038/nclimate1633.

11. Davison, G; Trouble Waters. Down the gurgler: Historical influences on Australian domestic water consumption; Troy, P., and Troy, P. N., Eds.; ANU E Press 2008, 37–65.

12. Gan, K., and Purss C.; Reducing non-revenue water in a retail water company. AWA OzWater Conference, 8-10 March 2010, Brisbane, Australia. 2010.

13. Girard, M., and Stewart, R. A.; Implementation of pressure and leakage management strategies on the gold coast, Australia: Case study. *J. Water Resour. Plan. Manage.* 2007, 133 (3), 210-217.

14. Guan, K.; Thompson, S. E.; Harman, C. J.; Basu, N. B.; Rao, P. S. C.; Sivapalan, M.; Packman, A. I., and P. K. Kalita; Spatiotemporal scaling of hydrological and agrochemical export dynamics in a tile-drained Midwestern watershed, *Water Resour. Res.*, 2011, 47, DOI:10.1029/2010WR009997.

15. Grant, S.; Fletcher, T. D.; Feldman, D; Saphores, J. D.; Cook, P. L. M.; Stewardson, M., and Low, K.; Adapting urban water systems to a changing climate: Lessons from the Millennium drought in southeast Australia. *Environ. Sci. Tech.,* 2013, 47, 10727–10734.

16. Grinsted, A.; Moore, J. C., and Jevrejeva S.; Application of the cross wavelet transform and wavelet coherence to geophysical time series. *Nonlinear Process. Geophys.,* 2004, 11, 561–566.

17. Haque, M.; Hagare, D.; Rahman, A., and Kibria, G. (2014). Quantification of Water Savings due to Drought Restrictions in Water Demand Forecasting Models. *J. Water Resour. Plann. Manage.*, 2014, 140(11); DOI: 10.1061/(ASCE)WR.1943-5452.0000423.

18. Haquea, M. M.; Egodawattac, P.; Rahmana, A; Goonetillekec, A.; Assessing the significance of climate and community factors on urban water demand. *Int. J. Sust. Built Env.,* 2015, 4(2), 222–230; DOI:10.1016/j.ijsbe.2015.11.001.

19. Helman, P.; Droughts in the Murray Darling basin since European settlement. GCCM Research Report No. 100, 2009; http://www.mdba.gov.au/kid/files/2265-DroughtsInMDBsinceEuropeanSettlement1.pdf.

20. Hoekstra, A. Y.; Mekonnen, M. M.; Chapagain, A. K.; Mathews, R. E., and Richter, B. D.; Global Monthly Water Scarcity: Blue Water Footprints versus Blue Water Availability. *PLoS ONE*, 2012, 7(2); DOI:10.1371/journal.pone.0032688.

21. Johnes, D. A.; Wang, William, and Fawcette, R.; High-quality spatial climate data-sets for Australia. *Aust. Meteorol. Ocean. J.,* 2009, 58, 233−248.

22. Keitt, T. H., and Urban, D. L.; Scale-specific inference using wavelets. Ecol. 2005, 86(9), 2497–2504; DOI: 10.1890/04-1016.

23. Leblanc, M. J.; Tregoning, P.; Ramillien, G., and Tweed, S. O.; Fakes A. Basin-scale, integrated observations of the early 21st century multiyear drought in southeast Australia. *Water Resour. Res.*, 2009, 45(4), 1−10.

24. Low, K. G.; Grant, S. B.; Hamilton, A. J.; Gan, K.; Saphores, J. D.; Arora, M., and Feldman, D. L. Fighting drought with innovation: Melbourne's response to the Millennium Drought in Southeast Australia. WIREs Water: Water 2015, 2(4), 315−328; DOI: 10.1002/wat2.1087.

25. National Water Commission. The National Water Initiative – Securing Australia's water future: 2011 assessment. Canberra: NWC. http://www.nwc.gov.au/__data/assets/pdf_file/0018/8244/2011-BiennialAssessment-full_report.pdf.

26. Oki, T., and Kanae, S.; Global Hydrological Cycles and World Water Resources. *Science*, 2006, 313 (5790), 1068-1072; DOI: 10.1126/science.1128845.

27. O'Neill, S.; Barnett, J.; Maladaptation. *Glob. Environ. Chang.,* 2010, 20, 211−213.

28. Pilgram, J. J. Australia's water resources. From use to management. CSIRO Publishing, Collingwood VIC, Australia, 2006.

29. Radcliffe, J. C.; Water recycling in Australia – during and after the drought. *Environ. Sci.: Water Res. Technol*., 2015, 1, 554−562.

30. Rosenblatt, H. M.; Spectral Analysis and Parametric Methods for Seasonal Adjustment, U. S. Bureau of the Census, working paper No. 23, Washington, D. C., 1965.

31. Secretarial Disaster Designations - 2016 Crop Year All Drought - Total Counties by State; United States Department of Agriculture 2016; http://www.fsa.usda.gov/Assets/USDA-FSA-Public/usdafiles/Disaster-Assist/Secretarials/2016-Secretarial-Disaster-Assistance-Assets/ALL_DROUGHT_CoList_CY2016.pdf.

32. Seawater desalination in Australia. Research Office, Legislative Council Secretariat, 2015.

33. Sheffield, J.; Wood, E. F., and Roderick, M. L.; Little change in global drought over the past 60 years. *Nature*, 2012, 491, 435–438; DOI:10.1038/nature11575.

34. Tiwari, M. K., Adamowski, J. F.; Medium-Term Urban Water Demand Forecasting with Limited Data Using an Ensemble Wavelet–Bootstrap Machine-Learning Approach. J. Water Resour. Plann. Manage., 2015, 141(2) ; DOI: 10.1061/(ASCE)WR.1943-5452.0000454.

35. Torrence, C., and Compo, G. P.; A Practical Guide to wavelet analysis. *Bull. Am. Meteorol. Soc.,* 1998, 79(1), 61−78; DOI: http://dx.doi.org/10.1175/15200477(1998)079<0061:APGTWA>2.0.CO;2.

36. Torrence, C., and Webster, P. J.; Interdecadal Changes in the ENSO–Monsoon System. *J. Clim.*, 1999, 12, 2679−2690.

37. Turner, S. W. D.; Marlow, D.; Ekstrom, M.; Rhodes, B. G.; Kularathna, U., and Jeffrey, P. J.; Linking climate projections to performance: A yield-based decision scaling assessment of a large urban water resources system. *Water Resour. Res.,* 2014, 50, 3553–3567; DOI: 10.1002/2013WR015156.

38. Ummenhofer C. C.; Gupta, A. S.; Briggs P. R.; England, M. H.; Mcintosh P. C.; Meyers, G. A.; Pook, M. J.; Raupach, M. R., and Risbey, A. J. S.; Indian and Pacific Ocean Influences on Southeast Australian Drought and Soil Moisture. *J. Clim.* 2011, 24, 1313–1336; DOI: 10.1175/2010JCLI3475.1.

39. Van den berg, C.; Drivers of non-revenue water: A cross-national analysis. *Util. Policy.* 2015, 36, 71-78.

40. Van Dijk, A. I. J. M.; Beck, H. E.; Crosbie, R. S.; de Jeu, R. A. M., and Liu, Y. Y.; The Millennium Drought in southeast Australia (2001–2009) : Natural and human causes and implications for water resources, ecosystems, economy, and society. *Water Resour. Res.* 2013, 49(2), 1040–1057; DOI: 10.1002/wrcr.20123.

41. van Leeuwen, C. J. Water governance and the quality of water services in the city of Melbourne. *Urban Water Journal.* 2015; DOI:10.1080/1573062X.2015.1086008.

42. Verdon-Kidd, D. C., and Kiem, A. S.; Nature and causes of protracted droughts in southeast Australia: Comparison between the Federation, WWII, and Big Dry droughts, *Geophys. Res. Lett.*, 2009, 36, 1−6.

43. Viggers, J.; Lindenmayer, D., and *Weaver, H.; Melbourne's water catchments: Perspectives on a world-class water supply;* CISRO Publishing: Collingwood, Australia, 2013.

44. Water outlook for Melbourne, 2014 https://www.yvw.com.au/yvw/groups/public/documents/document/yvw1004058.pdf.

45. Walsh, C. J.; Roy, A. H.; Feminellia, J. W.; Cottingham, P. D., Groffman, P. M.; Morgan, R. P.; The urban stream syndrome: current knowledge and the search for a cure. *J. N. Am. Benthol. Soc.*, 2005, 24(3), 706–723.

46. Walsh, C. J.; Booth, D. B.; Burns, M. J.; Fletcher, T. D.; Hale, R. L.; Hoang, L. N.; Livingston, G.; Rippy, M. A.; Roy, A. H.; Scoggins, M., and Wallace, A.; Principles for urban stormwater management to protect stream ecosystems. *Freshw. Sci*. 2016, 35, 398–411.

47. Wellman, K., and Spiller, M.; Urban Infrastructure: Finance and Management. Financing and Managing Urban Water; Wiley-Blackwell 2012, 149–177.

48. Westra, S., and A. Sharma; Dominant modes of interannual variability in Australian rainfall analyzed using wavelets, J. Geophys. Res., 2006, 111, 1−10; DOI:10.1029/2005JD005996.

49. Wilhite, D. A., Ed. Drought and water crises. Science, Technology, and Management Issues; CRC Press 2005, 173–190.

50. WSAA Water Services; Annual report; Water services association of Australia: 2011-2012; https://www.wsaa.asn.au/sites/default/files/publication/download/WSAA%20Annual%20Report%202011-2012.pdf.

51. Zhou, S. L.; McMahon, T. A.; Walton, A., and Lewis, J.; Forecasting daily urban water demand: A case study of Melbourne. *J. Hydrol.,* 2000, 236, 153–164, DOI: 10.1016/S0022-1694(00)00287-0.

APPENDIX A: SUPPLEMENTAL METHODS

Significance tests for wavelet power and coherence

Regions of significant power or coherence (black contour lines in **Figs. 2, and S3**) were identified using Monte Carlo analysis. Briefly, 10,000 synthetic red noise timeseries (X_{n+1}) were generated for rainfall (R), temperature (T), inflow (I), and consumption (C) as in EQ (1):

$$X_{n=1} = \sigma_X \sqrt{1 + r_1^2} Z_n$$

$$X_{n+1} = r_1 X_n + \sigma_X \sqrt{1 + r_1^2} Z_n \qquad \text{EQ (1)}$$

where n is an index spanning 1 to length X, r_1 is the lag-1 autoregressive coefficient for *R, T, I,* or *C*, σ_x is the standard deviation of X, and Z_n is a white noise process (e.g., randomly generated normal variable) with zero mean and unit variance. These red noise timeseries were used to generate frequency and time-specific null distributions for wavelet power and coherence from which an upper 95% confidence (CI) bound could be estimated (see below). All values of coherence or power from *R*, *T*, *I* or *C* data that exceeded this 95% CI bound were determined to be significant at a $p < 0.05$ level.

To estimate, the upper CI bound for spectral power, frequency and time-specific null distributions were generated by taking the continuous wavelet transform (CWT) of each red noise timeseries (as in Grinsted *et al*., 2004), generating 10,000 realizations of power for each time-frequency coordinate in each input timeseries (e.g., *R, T, I* or *C*). A similar approach was used to generate frequency and time-specific null distributions of coherence (e.g., between *R:T, R:I, R:C, T:I, T:C,* and *I:C*), save that coherence between pairs of rednoise timeseries was estimated in lieu of individual timeseries power (see Grinsted *et al*., 2004 for wavelet coherence

equations). A percentile approach was used to calculate the upper 95% confidence bound for each null distribution, where values comprising the null (coherence or power) were sorted, and the 9,500th value retained as the upper (95%) bound.

Discrete wavelet transformation and multiple linear regression

In practice, DWT is analogous to CWT in that it provides a complete representation of the original timeseries in time and frequency space, but differs in that the frequencies and timeframes (translations) evaluated are restricted to an orthonormal set.[2] This feature facilitates subsequent analyses like regression that require independence in time and scale, but comes at the cost of reduced signal fidelity (i.e., transient events and/or oscillatory behavior are harder to resolve). DWT uses simultaneous low and hi-pass filtering to repeatedly split a timeseries into detail coefficients, which capture variability at a given frequency, and approximation coefficients, which capture the remainder (e.g., lower frequency components) of the signal.[2,3] At each step, the wavelet coefficients are downsampled by a factor of two and the approximation coefficients passed on to be filtered again at a lower frequency. In our analysis we use the Haar wavelet as a high-pass filter (e.g., mother wavelet) and the corresponding Haar scaling function as a low-pass filter (e.g., father wavelet) for *R*, *T*, *I*, and *C*, as in Keitt *et al*., 2005.

Once wavelet coefficients were obtained through DWT for each timeseries, the following steps were taken in order to construct a best-fit regression model for *C* using climate variables (see **Fig. S2**): 1) universal thresholding was applied to the wavelet coefficients of *R*, *T*, *I*, and *C* to reduce noise, as recommended by Westra *et al.*, 2006; 2) the variance inflation factor (VIF) was calculated for *R*, *T*, and *I* at each frequency to identify multicolinearity (variables with VIF > 5 at a given frequency were excluded from the regression at that frequency); 3) MLR was

performed for each frequency band, where the dependent variable was *C* and the independent variables were *R*, *T*, *I,* and their pairwise interaction terms: functional marginality was invoked so that no models included interaction terms without first including both parent variables; 4) The best model for each frequency was selected using Akaike's Information Criterion, corrected for small sample sizes, and 5) these models were compiled to construct an optimal climate model across all frequencies. After characterizing our optimal climate model in time-frequency space, an inverse DWT was used to recover the synthetic consumption timeseries represented by the model. CWT was then performed on both modeled and observed consumption: the residual (observations – model) was evaluated for time-frequency regions not well explained by climate that could reflect anthropogenic controls on urban water consumption.

Significance tests for long-term trends in phase: non-parametric bootstrapped regression

Non-parametric bootstrap statistics were used to estimate 95% confidence intervals for the slope of the long term trend in phase lag (estimated at an annual frequency) across all combinations of *R*, *T*, *I*, and *C* between 1940 and 2012 (trends are shown in **Fig. 2**). A residual-based resampling (or fixed *x*) approach was employed for this analysis (as in Azizian *et al*., 2015). Briefly, a first order polynomial was fit to each phase lag timeseries (e.g., *Lag* (*y* values) and *year* (*x* values). The residuals were calculated and bootstrapped 10,000 times, producing 10,000 realizations of error. Each realization of error was added to the original linear fit and then re-fit. The slope estimates from these 10,000 fits were retained, and used to calculate 1) the average slope and 2) 95% confidence intervals about that average. Because the probability distribution of the slopes was observed to be symmetric, confidence intervals were calculated using a basic percentile approach where all 10,000 slope estimates were sorted and the 250th and 9,750th values retained

as the lower (2.5%) and upper (97.5%) confidence bounds, respectively.

SUPPLEMENTAL REFERENCES

1) Grinsted, A.; Moore, J. C., and Jevrejeva S.; Application of the cross wavelet transform and wavelet coherence to geophysical time series. *Nonlinear Process. Geophys.,* **2004**, 11, 561–566.

2) Westra, S., and Sharma, A.; Dominant modes of interannual variability in Australian rainfall analyzed using wavelets, *J. Geophys. Res.,* **2006**, *111*, 1−10; DOI:10.1029/2005JD005996.

3) Keitt, T. H., and Urban, D. L.; Scale-specific inference using wavelets. *Ecol.* **2005**, *86*(9), 2497−2504; DOI: 10.1890/04-1016.

4) Azizian, M.; Grant, S.; Kessler, A.; Cook, P.; Rippy, M. A.; Stewardson, M. Bedforms as biocatalytic filters: a pumping and streamline segregation (PASS) model for nitrate removal in permeable sediments. *Environmental Science & Technology*. **2015.** *49*, 10993–11002 DOI:10.1021/acs.est.5b01941.

APPENDIX B: SUPPLEMENTAL FIGURES

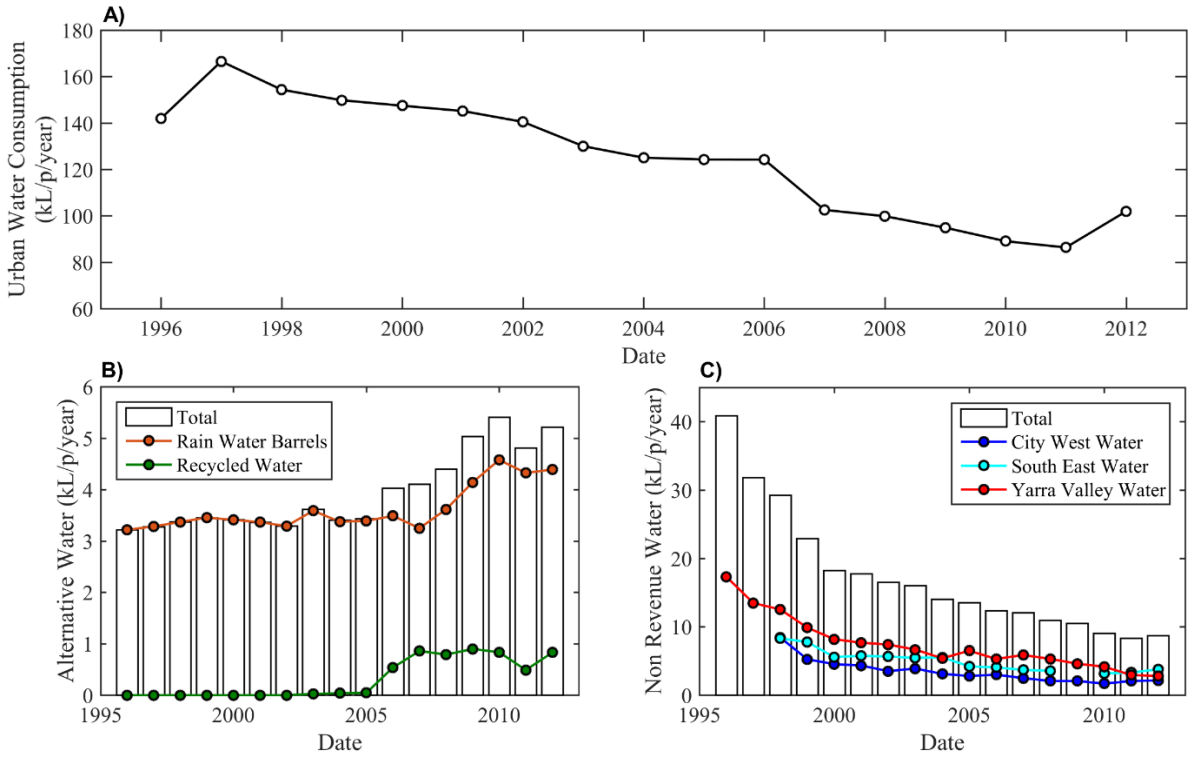

Figure S1: Annual timeseries of (**A**) per capita urban water consumption (kL/p/y), (**B**) per capita water volume from alternative sources (kL/p/y), and (**C**) per capita non revenue water (NRW) between 1995 and 2012. Total per capita NRW and alternative water volume are shown using white bars (**B, C**). Each total is broken into multiple components: rain water barrels (orange) and recycled water (green) for alternative water sources (**B**), and by retailer (e.g., City West Water (blue), South East Water (cyan) and Yarra Valley Water (red)) for NRW (**C**).

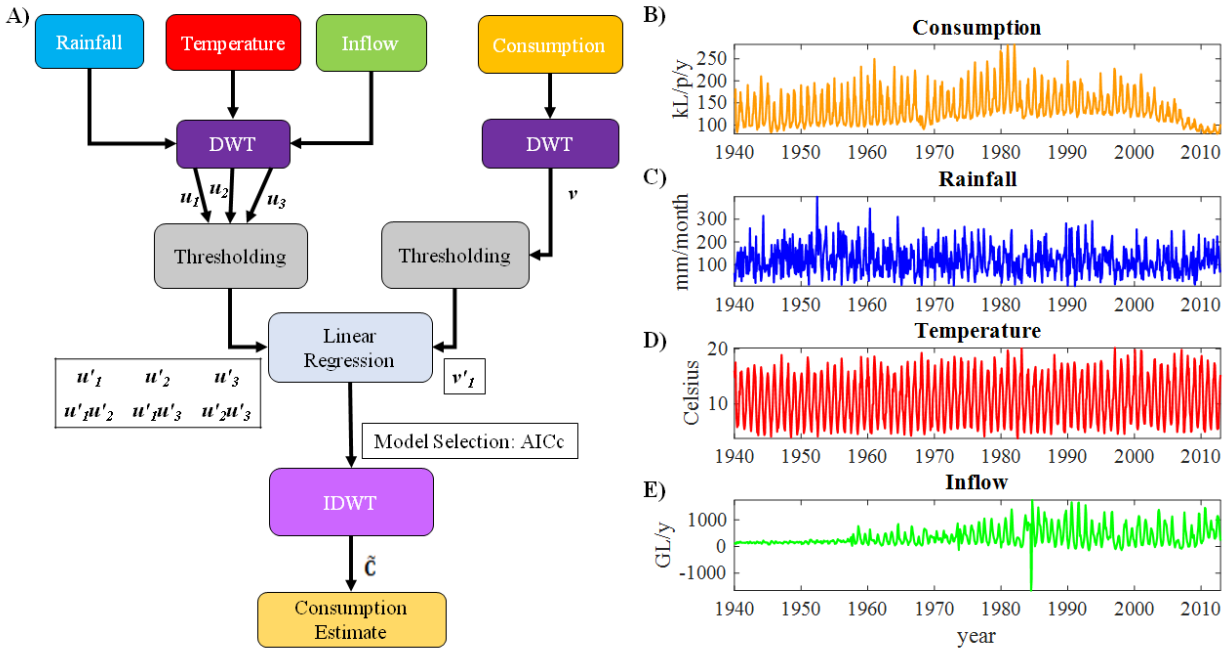

Figure S2: (**A**) A flow diagram of the combined discrete wavelet transform (DWT) and multiple linear regression (MLR) procedure used to construct our climate-forced consumption model: 1) DWT was used to generate frequency-dependent timeseries of wavelet coefficients for each dependent variable (rainfall (u_1; blue), temperature (u_2; red), and inflow(u_3; green)) and our independent variable (consumption (v_1; yellow)), 2) universal thresholding was applied to all wavelet coefficients generating de-noised coefficients u'_1, u'_2, u'_3, v'_1, 3) MLR was performed at each frequency using all combinations of dependent variables and their pairwise interaction terms (u'_1, u'_2, u'_3, $u'_1u'_2$, $u'_1u'_3$, $u'_2u'_3$), 4) the best frequency-specific model for v'_1 was selected using Akaike's information criterion corrected for small sample sizes (AICc), and 5) inverse DWT was performed on the compilation of all best fit frequency-specific models, recovering a best-fit consumption timeseries ($\tilde{\mathbf{C}}$). (**B-E**) Raw timeseries (e.g., prior to de-meaning and de-trending) of all dependent and independent variables used as inputs in our climate-only model: (**B**) consumption, kL/p/y; (**C**) rainfall, mm/month; (**D**) temperature, Celsius; and (**E**) inflow, GL/y.

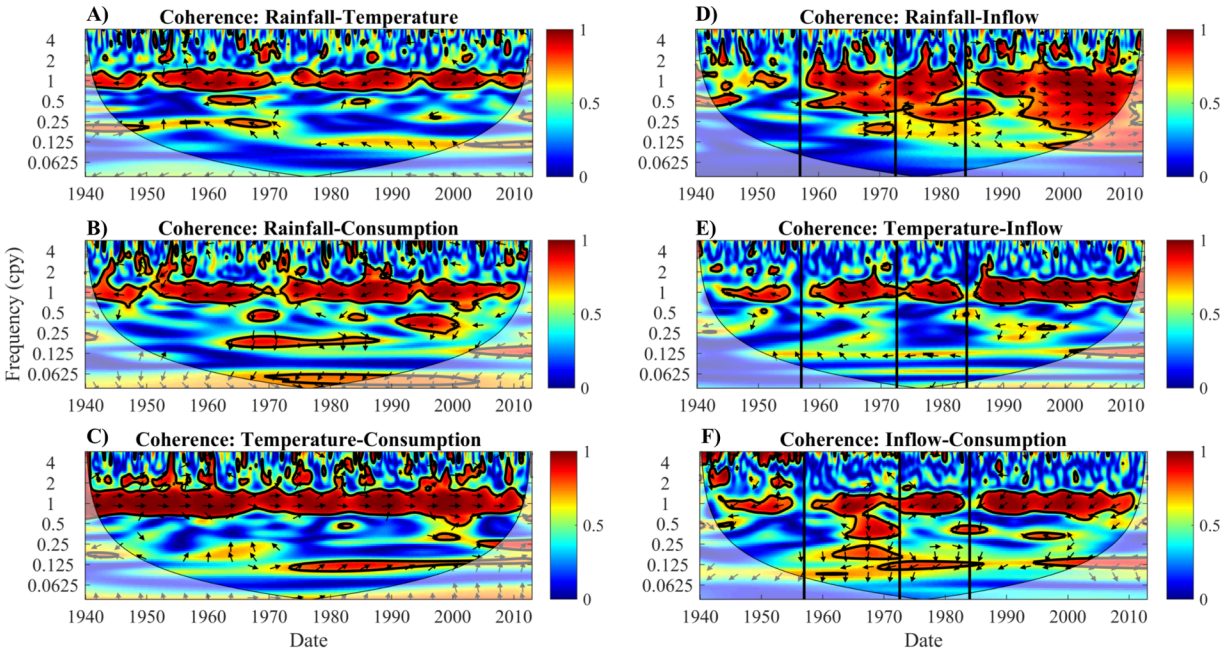

Figure S3: Contour plots of wavelet coherence (color) between (**A**) rainfall and temperature, (**B**) rainfall and consumption, (**C**) temperature and consumption, (**D**) rainfall and inflow, (**E**) temperature and inflow, and (**F**) inflow and consumption. Time (years) is on the *x*-axis, and frequency (cpy) is on the *y*-axis. Thick black contours denote regions of significant coherence ($p < 0.05$ level), and white shading (e.g., the cone of influence) indicates regions where coherence estimates are unreliable. Arrows denote phase relationships between variables: down (up) denotes variable 1(2) leading variable 2(1). Perfectly horizontal arrows indicate relationships that are totally in phase (pointing right) and out of phase (pointing left), respectively. Note that black vertical lines in (**D-F**) mark reservoir additions, including (from left to right) the Upper Yarra, Cardinia, and Thomson reservoirs.

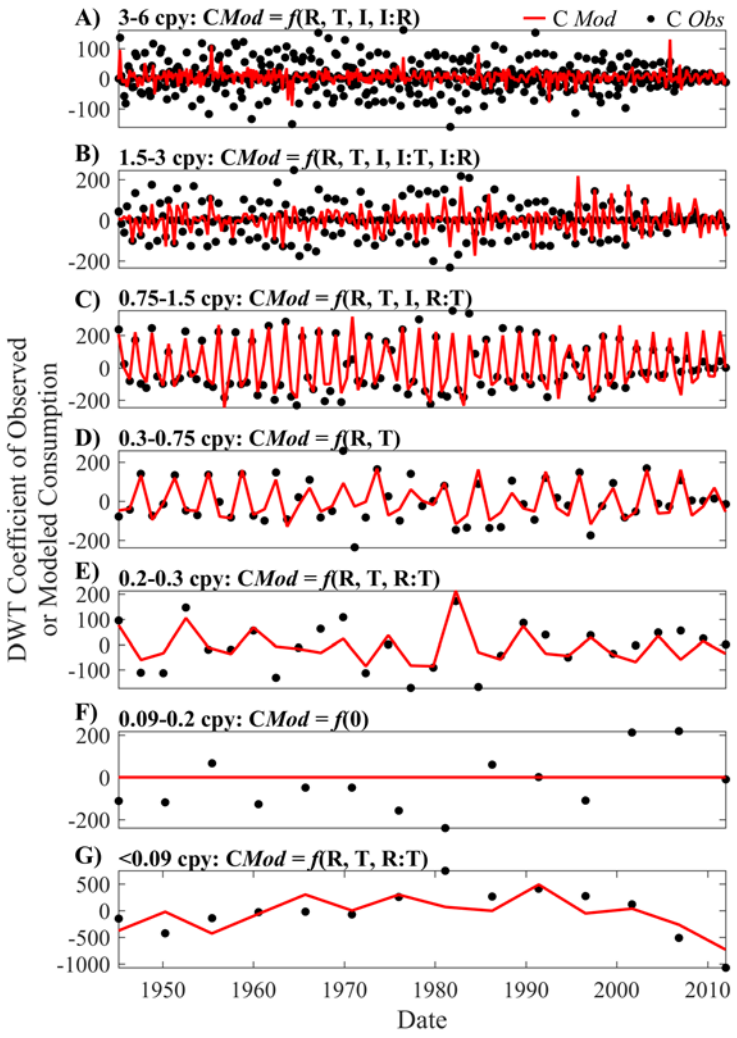

Figure S4: Timeseries of the frequency-specific model fits that comprise our overall best-fit climate model. Time (years) is on the *x*-axis, and the observed (black dots) or modeled (red line) magnitude of wavelet coefficients for consumption is on the *y*-axis. Panels correspond to different frequency bins: (**A**) 3-6 cpy, (**B**) 1.5-3 cpy, (**C**) 0.75-1.5 cpy, (**D**) 0.3-0.75 cpy, (**E**) 0.2-0.3 cpy, (**F**) 0.09-0.2 cpy, and (**G**) < 0.09 cpy. The parameters included in the best-fit model for each frequency bin are listed at the top of its respective panel.

APPENDIX C: SUPPLEMENTAL TABLES

Table S1: Temporal Trends in Phase Relationships Between R, T, I, and C

Timeseries	**Avg. Lead (months) *(SD)***	**Slope: Long Term Trend in Lead (days/year) *(99% CI)***	**Total ΔLead: 1940 to 2012 (months) *(99% CI)***
R leads T	5.3 *(0.5)*	-2.8 *(-3.7,-1.8)* **	-0.6 *(-0.7, -0.4)*
I leads T	4.8 *(0.4)*	-4.5 *(-5.1, -4.0)***	-0.9 *(-1.0, -0.8)*
R leads C	5.2 *(0.5)*	-2.9 *(-3.7, -2.2)***	-0.6 *(-0.7, -0.4)*
I leads C	4.7 *(0.4)*	-4.5 *(-5.1, -4.0)***	-0.9 *(-1.0, -0.8)*
R leads I	0.4 *(0.5)*	3.1 *(2.2, 4.0)***	0.6 *(0.4, 0.8)*
T leads C	0.1 *(0.2)*	0.3 *(0.0, 0.4)**	0.1 *(0.0-0.1)*

**: slope significantly different than 0 at the $p < 0.001$ level

*: slope significantly different than 0 at the $p < 0.01$ level

Table S2: Frequency-specific Model Fits

Frequency Band (cpy)	***k***	**Model Variables**	***Coef***	**wAICc (%)**	**% VE**
3-6	5	Intercept*	5.4	22	19
		R*	-0.33		
		T*	69		
		I	-3.6×10^{-2}		
		I:R*	-9.2×10^{-4}		
1.5-3	5	R*	-0.47	52	51
		T*	61		
		I	-3.6×10^{-2}		
		I:R	-5.4×10^{-4}		
		I:T*	-8.5×10^{-2}		
0.75-1.5	4	R*	-0.81	17	83
		T*	20		
		I	2.7×10^{-2}		
		R:T*	5.8×10^{-2}		
0.3-0.75	3	Intercept*	-27	25	71
		R*	-0.39		
		T*	24		
0.2-0.3	4	Intercept*	-36	37	56
		R*	-0.72		
		T*	69		
		R:T*	0.65		
0.09-0.2	1	Intercept	0	29	2
<0.09	3	R*	-2.9	25	52
		T*	56		
		R:T*	2.3		

*: significant at a $p < 0.05$ level